

# The Calibration Process of Building Energy Models

Roberta Perneti, Alessandro Prada and Paolo Baggio

**Abstract** The importance of model calibration has been growing up as a result of the energy refurbishment policy promoted by the recast Energy Performance of Buildings Directive (EPBD 2010/31/EU). In fact, with the purpose of ensuring a suitable refurbishment design with effective energy conservation measures (ECM), an accurate model has to be defined in order to assess the energy behaviour of the as-built building. In this chapter, some issues related to the model calibration are presented, starting from the definition of an operative procedure step by step. Furthermore, for the most critical phases of the procedure, analysis techniques and experimental methods are described both through theory and practical examples. Finally, throughout the chapter, the analysis of a case study is presented.

## Nomenclature

$CDH_{26}$	Cooling degree hours at a base temperature of 26 °C
$F$	Sensitivity index for factorial method
$HDH_{18}$	Heating degree hours at a base temperature of 18 °C
$k$	Specific heat capacitance ( $J m^{-2} K^{-1}$ )
$n$	Number of simulation steps
$s$	Sensitivity index for differential sensitivity analysis
$R^2$	Regression index

---

R. Perneti (✉)

University of Pavia, Via Ferrata 1, 27100 Pavia, Italy

e-mail: roberta.perneti@unipv.it

A. Prada

Faculty of Science and Technology, Free University of Bozen/Bolzano,  
piazza Università 5, 39100 Bolzano, Italy

e-mail: alessandro.prada@unibz.it

P. Baggio

Department of Civil Environmental and Mechanical Engineering,

University of Trento, via Mesiano 77, 38123 Trento, Italy

e-mail: paolo.baggio@unitn.it

$U$	Thermal transmittance ( $\text{W m}^{-2} \text{K}^{-1}$ )
$O_j$	Model response of the $j^{\text{th}}$ simulation

### Greek Symbols

$\Lambda$	Thermal conductance ( $\text{W m}^{-2} \text{K}^{-1}$ )
$\theta$	Dry bulb temperature (K)

### Subscripts

$C$	Cooling
$f$	Floor
$H$	Heating
$I$	Internal
$r$	Roof
sim	Simulated
set	Set point
$w$	Wall

## 1 Introduction

Energy simulation represents a useful tool to describe actual building behaviour; hence, it is applied not only in the design process but also in the post-occupancy analysis. In this case, the purpose is the evaluation of building actual energy efficiency in order to estimate the potential energy savings of existing constructions. In fact, the recast Energy Performance of Buildings Directive (EPBD [28] 2010/31/EU) highlights that residential and commercial buildings account for more than one-third of total annual energy consumption. Since significant energy savings can be achieved through energy conservation measures (ECM) for existing building stock, the importance of refurbishment has been growing. Consequently, simulations have been applied to the existing constructions to assess their energy performance and to define effective ECM. In this regard, dynamic energy simulation allows to understand the dynamic interactions between climate, building, occupants and energy systems. However, the large number of required inputs and parameters affects the reliability of dynamic simulation and significant discrepancies between predicted and real data could occur. Furthermore, the comparison between actual consumption and quasi-steady state prediction highlights important deviations. For these reasons, model calibration with monitored data is often appropriate in order to refine models and to develop more realistic energy-behaviour simulations.

Model calibration is widely used for commercial and office buildings analyses, which require the definition of complex transient simulations in order to design effective ECM. In fact, due to the large dimensions of these buildings and the

operational daily schedules that vary with hourly interval, dynamic simulations are necessary to assess reliable energy behaviour.

Nevertheless, model calibration could be applied even for residential buildings. Quasi-steady state simulations usually require limited in situ measurements for model calibration, and they provide for the general behaviour of constructions (most of all with monthly intervals). Moreover, the input data are similar to the parameters employed in energy labelling, and the model calibration can be performed with utility bills. Consequently, this kind of evaluation is not time-consuming, and it guarantees for economical sustainability. Therefore, quasi-steady state simulations represent a useful tool for energy performance evaluation of both average- and small-dimension buildings.

On the other hand, a different approach is suitable for large-dimension houses, whose typology often constitutes social housing and it is widely spread in the suburbs of all the European cities. These constructions need a general refurbishment, most of all in terms of energy requirements, and they represent one of the strategic targets of EPBD [28] 2010/31/EU, because of the significant potential savings. In this regard, a large-scale evaluation as well as important investments are necessary for a general energy renewal. Thus, transient simulations can represent an important tool to plan effective ECM. Finally, time and economical costs due to dynamic models are sustainable in relation to these construction dimensions and to the potential energy savings.

Therefore, even in this case, model calibration is necessary in order to define an accurate model of the ‘as-built’ building and to design effective ECM.

According to these considerations, the large application field of model calibration requires operative procedures. A new European standard is going to be developed by CEN Technical Committee 89 (Working Group 14), and it will provide for calibration strategies and measurements of post-processing procedures for building energy models [24]. Currently, three protocols define general criteria and tolerance ranges for model calibration:

- International Performance Measurement and Verification Protocol (IPMVP [27]),
- Measurement and Verification (M&V Guidelines [31]);
- ASHRAE Guideline 14/2002: Measure of energy and demand savings [21].

However, none of these standards define an operative procedure to calibrate building models. In the literature, several studies deal with the model calibration issues using actual energy consumption either from in situ monitoring during the calibration period (e.g., [10, 12]) or from the analysis of monthly utility bills (e.g., [20]). Only a few works adopt the internal temperature as a calibration goal (e.g., [16]). In fact, this approach could be affected by a series of uncertainties and interactions with the indoor environment: occupant behaviour, internal gain and building equipment. Besides, the measurement of several variables can be an expensive and time-consuming activity. However, the model calibration using temperature as a control variable is the only viable procedure when no operating HVAC systems are present in a building.

Finally, the aim of model calibration is to minimize the discrepancies between the model and the real behaviour of buildings, therefore an extended procedure is necessary.

## 2 The Calibration Approach

Model calibration is an iterative process that aims to reduce the discrepancies between simulated and actual building energy behaviour, through the refinement of the model parameters.

In order to ensure the reproducibility of the calibration process and to reduce the uncertainties of model predictions, it is necessary to establish a reference procedure that defines the operative methodologies and the evaluation criteria of building properties. The calibration protocol presented and applied in this chapter is defined for existing buildings. It is compounded by several phases as shown in Fig. 1.

### 2.1 Preliminary Operations

The first step of a calibration process is the definition of scope and application field. In this chapter, a procedure for the calibration of existing building energy models is reported. During the early stage of the analysis, it is fundamental to check whether fuel measurement devices are available for the HVAC systems. Otherwise, the possibility of experimental equipment installation (for short- or long-term measures) should be investigated. Nevertheless, if a direct measure is not possible, building energy consumption can be derived from the utility bills, with a lower accuracy level respect to direct measurement.

### 2.2 General Data Gathering and Base Model Definition

The definition of a simulation model requires a large number of input data:

- *Building features*: dimensions and thermophysical properties of materials
- *HVAC system*: typology and technical features of the subsystem appliances, schedules and control strategies
- *Operating conditions*: internal gains due to lighting, equipments and people, zone occupancy and set point temperatures
- *Weather data*: dry bulb temperature, solar radiation, relative humidity and wind speed evaluated at the building location.

These data are used for the development of the base reference model. This model is defined using the real features and dimensions of building collected

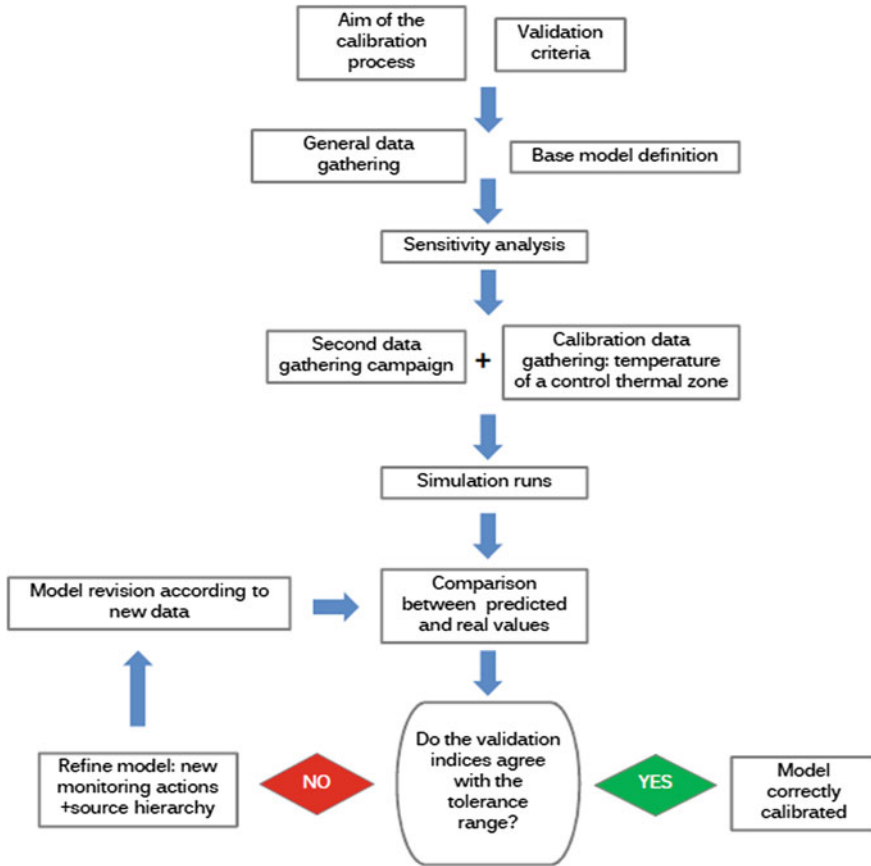


Fig. 1 Model calibration process

through a geometrical relief. Furthermore, for all the other parameters, standard reference values are used. This base model does not reproduce reliable energy behaviour of the building, but it represents the reference simulation for carrying out the sensitivity analysis (SA).

### 2.3 Sensitivity Analysis

The SA aims to evaluate the influence of input data on the dependant variables that, in case of building simulation, represent the energy behaviour of constructions (consumption and temperature trends).

The SA could be carried out with several methods, which are expounded in Sect. 4.

## 2.4 *Second Data Gathering Campaign and Simulation Runs*

During this phase of the calibration process, two categories of data are collected:

- Model input
- Control variables for calibration

The measurement of real values for the control variables for calibration allows to assess the reliability of the model during the validation step.

On the other hand, the gathering of model input for building simulation is highly complex due to the large amount of parameters that can affect the model results. Therefore, it is necessary to define strict criteria for the data selection. The SA highlights the most influent parameters and inputs that have to be investigated to obtain an effective simulation. Moreover, in order to refine the model, a source hierarchy has to be defined as explained in [Sect. 5](#).

Finally, a series of simulations is carried out considering different inputs and boundary conditions.

## 2.5 *Calibration Criteria*

The discrepancies between real measured control parameters and model results have to be evaluated through given validation criteria, which assess the level of model calibration. In this phase, the indices and the tolerance range for the reliability assessment have to be defined.

## 2.6 *Model Validation*

In this phase, the model outputs are compared to the actual values of control variables for model calibration. If the results respect the calibration criteria, the model is correctly defined, otherwise it has to be refined by changing the model parameters or through a new data collection campaign, carried out according to the source hierarchy.

Finally, the calibrated model must be validated over a different measurement period respect to those used for the calibration phase. In fact, the calibration of the simulation model is a so-called inverse heat transfer problem, for which the uniqueness of the solution cannot be taken for granted [11].<sup>1</sup>

---

<sup>1</sup> “Inverse Heat Transfer Problems (IHTP) rely on temperature and/or heat flux measurements for the estimation of unknown quantities appearing in the analysis of physical problems in thermal engineering. As an example, inverse problems dealing with heat conduction have been generally associated with estimation of unknown boundary heat flux, by using temperature measurement taken below the boundary surface. Therefore, while in the classical direct heat conduction problem the cause (boundary heat flux) is given and the effect (temperature field in



**Fig. 2** a North-east facade. b North-west facade

### 3 Case Study

The case study is a historical manufacturing facility built in Rovereto in Northern Italy. The building, presently disused, was realized in 1854 as a storage construction for the tobacco processing (Fig. 2).

It has an overall surface of 3,650 m<sup>2</sup>, four levels, one basement and a flat roof with a black coating (absorption coefficient roughly equal to 0.9).

The building has a concrete structure (beam and pillar) and a massive envelope made of stone and bricks, whose thickness ranges from 90 cm of the underground floor to 65 cm of the third floor. Except for the underground level, which is characterized by basement windows, the envelope has a homogeneous ratio of glazing over opaque surface equal to 30 %.

The windows have timber frames with single glazing. During the relief, several leakages in the glass elements were detected, with the consequence of significant infiltration rates.

The building is now disused, and therefore, it has no operating HVAC systems.

Considering the high thermal capacitance of the internal walls, each room is modelled as a single thermal zone, as shown in Figs. 3 and 4.

The envelope material properties are unknown, and there are no available design documentations. Therefore, according to the building features, the construction year, the structure and the thickness, and standard compositions were extracted from the Appendix A of the Italian technical specification UNI/TS 11300-1 [30] (Table 1).

### 4 Sensitivity Analysis of Building Energy Model

The detailed modelling of the building and HVAC energy performances leads to careful study of the interactions between the envelope, the occupants, internal loads and energy systems. However, the increasing detail of the models requires a

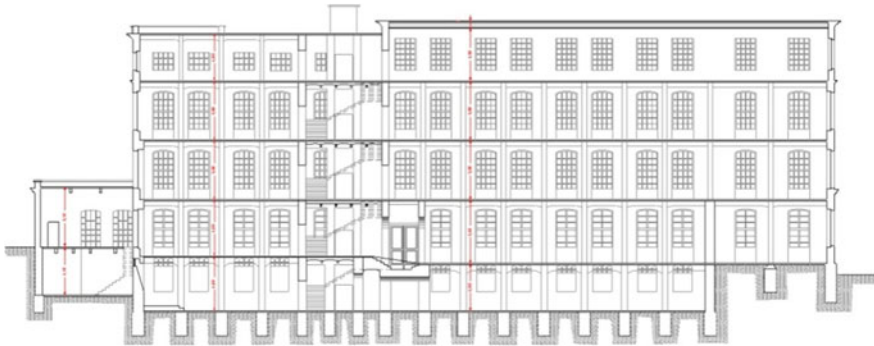
---

(Footnote 1 continued)

the body) is determined, the inverse problem involves the estimation of the cause from the knowledge of the effect” (Ozisik and Orlande 2000).



**Fig. 3** Thermal zones



**Fig. 4** Building section

greater number of input data that, if not properly investigated, can undermine the reliability of results. Furthermore, the relative influence of stochastic variations in building energy needs increases for low energy constructions. On the other hand, the input data do not affect in the same way the model predictions and, in this sense, it is important to carefully assess the sensitivity of the model to the input parameters.

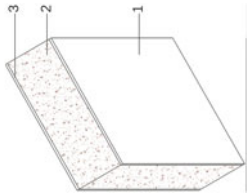

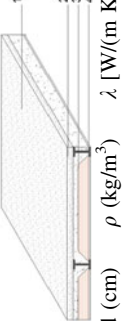
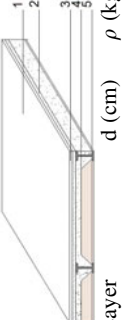
A practical definition is that SA is an answer to the questions ‘To what extent simulation predictions are reliable if input data are affected by uncertainty or are known with certain accuracy?’ or ‘To what extent the accuracy and the precision of model previsions improve if the knowledge of the input data is increased?’

A more precise definition is provided by Kioutsioukis et al. [5], which defines the SA as ‘the study of how uncertainty in the output of a model (numerical or otherwise) can be apportioned to different sources of uncertainty in the model input’.

The main application of the SA in the calibration of the building energy model thus becomes the identification of the critical inputs for the results reliability. This knowledge allows to establish priorities and to limit the experimental activities for input data measurements. In this way, it will be possible to minimize the in situ measures, which can become time-consuming activities.



**Table 1** Envelope composition

		Brick and stone wall			Ground floor				
									
Layer	d (cm)	$\rho$ (kg/m <sup>3</sup> )	$\lambda$ [W/(m K)]	R (m <sup>2</sup> K/W)	Layer	d (cm)	$\rho$ (kg/m <sup>3</sup> )	$\lambda$ [W/(m K)]	R (m <sup>2</sup> K/W)
1 Internal plaster	2	1,400	0.700	-	1 Mortar	3	2,000	1.470	-
2 Brick and stones	30-65	1,500	0.900	-	2 Concrete	10	2,000	1.400	-
3 External plaster	2	1,800	0.900	-	3 Stones	20-40	1,700	1.160	-
		Intermediate floor			Plain roof				
									
Layer	d (cm)	$\rho$ (kg/m <sup>3</sup> )	$\lambda$ [W/(m K)]	R (m <sup>2</sup> K/W)	Layer	d (cm)	$\rho$ (kg/m <sup>3</sup> )	$\lambda$ [W/(m K)]	R (m <sup>2</sup> K/W)
1 Mortar	2	2,000	1.400	-	1 Coating	1.5	1,200	0.170	-
2 Light concrete	9	400	0.150	-	2 Mortar	2	2,000	1.400	-
3 Hollow brick	6	600	-	0.250	3 Light concrete	9	400	0.150	-
4 Plaster	2	1,800	0.900	-	4 Hollow brick	6	600	-	0.250
					5 Plaster	2	1,800	0.900	-

Although in the literature there are several techniques for the SA [15], this chapter only describes a few simple techniques applied to building energy models, by highlighting the advantages and application limits.

As reported by Macdonald [8], the SA can be divided in two categories:

- *External methods*: where a sample of input is generated and, subsequently, the deterministic numerical model is executed for each input.
- *Internal methods*: that directly evaluates the output distribution from the uncertain inputs and from the differential equations of the mathematical model.

The external procedures are also divided in two branches, i.e., local and global. In local methods, the output uncertainty is evaluated with respect to changes around a specific value of individual parameters, whereas global methods quantify the output variation along a specific range of input variability.

The two approaches adopted in this chapter belong to the local methods based on the derivatives techniques, which have the advantage of being very efficient computationally with respect to global sensitivity methods such as Monte Carlo technique. In fact, derivative methods require only few simulations compared with the Monte Carlo methods. However, the main drawback is the limited suitability for models of unknown linearity. In fact, derivative methods provide punctual information about the model sensitivity (i.e., local method) and they do not allow an extrapolation of the results to the rest of the input space. In non-linear models, therefore, the impossibility to extend the results to other input values, with respect to those used for the estimation of the local sensitivity index, requires a reliable estimation of the input and of its expected variability range. These data must, therefore, be derived from the experience of the energy modeller thus to assure useful results from the SA.

The two techniques adopted in this chapter (local techniques based on the derivatives) do not represent the most detailed ones, but rather they could be easily integrated in energy simulations and, therefore, they are more useful for the application to real cases. Indeed, the ratio of an output  $O$  over an input  $I$  can be thought as a mathematical definition of the sensitivity of output model with respect to input variability.

## ***4.1 Differential Sensitivity Analysis***

The differential sensitivity analysis (DSA) is the backbone of local methods, and it works by perturbing an input data around the mean value while all the other parameters remain fixed [7]. For each perturbed value, the numerical simulation is carried out and the model response is calculated. Due to its robustness and simplicity, the DSA is the most diffuse method for a local uncertainty evaluation. The effects of an uncertain parameter are estimated by comparing the results of these

simulations against those with unperturbed inputs. Consequently, a sensitivity index ( $s$ ) of the model prediction to the uncertain parameter is defined as:

$$s = \frac{\Delta O}{\Delta I} \tag{1}$$

where  $\Delta O$  is the difference between the output with perturbed input with respect to deterministic model as well as  $\Delta I$  is the perturbation of input.

Since the sensitivity index depends on both the input and output dimensions, Lam and Hui [6] proposed a dimensionless index ( $s_{\%}$ ) defined as:

$$s_{\%} = \frac{\Delta O / O_{\text{base}}}{\Delta I / I_{\text{base}}} \tag{2}$$

where the numerator and denominator report, respectively, the percentage changes of output and input of the model.

The main weakness of this calculation procedure is that it assumes the perfect independency among all parameters. Consequently, only the elementary effect of each parameter could be computed while the combined effects can be estimated by a superposition in linear problems.

## 4.2 Factorial Methods

With the aim of overcoming DSA issues, the factorial method (FM) is also used in SA. The FM is a further development of the DSA approach that includes the interactions between parameters and, consequently, it permits the estimation of the higher-order effects. In this procedure, all the uncertain parameters are perturbed simultaneously around their mean values.

Usually, two different perturbation levels are considered for each parameter by imposing a low and high level (Table 2). In general,  $k$  parameters would require  $2^k$  simulations to generate all combinations for a full factorial simulation plan. These combinations represent the corners of the  $k$ -dimensional hypercube. Hence, the drawback of this technique is the number of simulations required that increase faster with the number of inputs.

If the factorial design of simulation aims to determine the model behaviour at a grid of locations inside the hypercube, more than 2 levels for each parameter are required. In this case, the total number of simulations becomes  $l^k$ , where  $l$  is the number of perturbation levels.

Based on the model predictions, the first-order effects can be calculated as:

$$F_A = \frac{(O_2 + O_4 + O_6 + O_8) - (O_1 + O_3 + O_5 + O_7)}{4} \tag{3}$$

$$F_B = \frac{(O_3 + O_4 + O_7 + O_8) - (O_1 + O_2 + O_5 + O_6)}{4} \tag{4}$$

**Table 2** Factorial design for three inputs with two perturbation levels

Number	A	B	C	A-B	A-C	B-C	A-B-C
1	-	-	-	+	+	+	-
2	+	-	-	-	-	+	+
3	-	+	-	-	+	-	+
4	+	+	-	+	-	-	-
5	-	-	+	+	-	-	+
6	+	-	+	-	+	-	-
7	-	+	+	-	-	+	-
8	+	+	+	+	+	+	+

$$F_C = \frac{(O_5 + O_6 + O_7 + O_8) - (O_1 + O_2 + O_3 + O_4)}{4} \quad (5)$$

where  $F_i$  is the first-order effect due to the  $i^{\text{th}}$  input and  $O_j$  represents output of the  $j^{\text{th}}$  simulation run.

The higher-order effects can be computed starting from the simulation runs. In this regard, the signs to be used in the following equations are obtained by multiplying the sign reported in (Table 2)

$$F_{A-B} = \frac{(O_1 + O_4 + O_5 + O_8) - (O_2 + O_3 + O_6 + O_7)}{4} \quad (6)$$

$$F_{A-C} = \frac{(O_1 + O_3 + O_6 + O_8) - (O_2 + O_4 + O_5 + O_7)}{4} \quad (7)$$

$$F_{B-C} = \frac{(O_1 + O_2 + O_7 + O_8) - (O_3 + O_4 + O_5 + O_6)}{4} \quad (8)$$

$$F_{A-B-C} = \frac{(O_2 + O_3 + O_5 + O_8) - (O_1 + O_4 + O_6 + O_7)}{4} \quad (9)$$

where  $F_{A-B}$  is the second-order effect due to the  $A^{\text{th}}$  and  $B^{\text{th}}$  inputs.

In the next section, the SA on the test case presented in Sect. 3 is reported. In particular, this analysis is carried on as a preliminary investigation of the hourly energy simulation model with the purpose of understanding the extent to which each parameter can affect the calibration procedure. Starting from this information, some of these inputs are further investigated by experimental activity or using a higher hierarchy source.

### 4.3 Example

In this section, the results of the SA on the case study described in Sect. 3 are presented. Since in the test case there is no energy systems, the dependent variables are related to the air temperature of the control thermal zone (i.e., P3\_Z1).

Besides, four different variables are adopted with the purpose of analysing some indexes closely related to system sizing and to the estimation of energy needs. In particular, the variables adopted are as follows:

- Minimum zone air temperature ( $t_{\min}$ )
- Maximum zone air temperature ( $t_{\max}$ )
- Zone Heating Degree Hour (HDH<sub>18</sub>)
- Zone Cooling Degree Hour (CDH<sub>26</sub>)

Heating and Cooling Zone Degree Hour indicate the sum of hourly difference between internal set point temperature (i.e., 18 °C for heating and 26 °C for cooling) and the simulated values of air temperature in the thermal zone.

$$\text{HDH}_{18} = \sum_{i=1}^n (\vartheta_{i,H,\text{set}} - \vartheta_{i,H,\text{sim}}) \quad (10)$$

$$\text{CDH}_{26} = \sum_{i=1}^n (\vartheta_{i,C,\text{sim}} - \vartheta_{i,C,\text{set}}) \quad (11)$$

These indices are adopted because they are proportional to the heating and cooling demand, as well as minimum and maximum temperature are closely related to the required size of energy system.

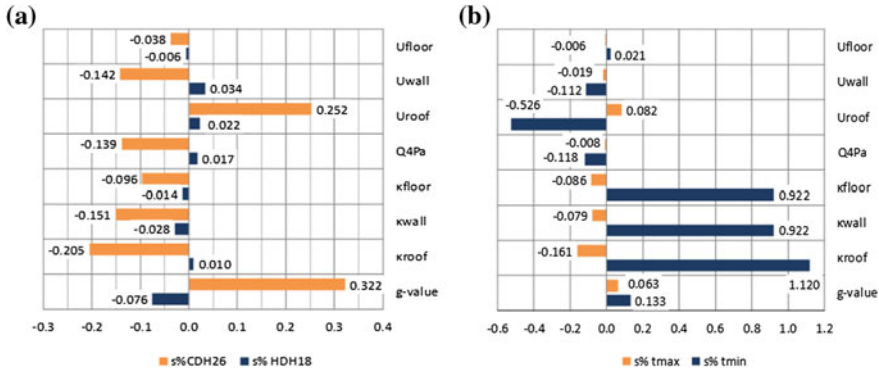
Starting from this point, a SA is carried out with a local external approach using both the DSA and the FM approaches. Based on some analyses about the uncertainty level of some parameters, the SA is performed by perturbing the following:

- External envelope air tightness expressed as an airflow for pressure difference of 4 Pa (Q4 Pa)
- Roof thermal transmittance ( $U_{\text{roof}}$ )
- Wall thermal transmittance ( $U_{\text{wall}}$ )
- Intermediate Floor thermal transmittance ( $U_{\text{floor}}$ )
- Roof thermal specific capacitance ( $\kappa_{\text{roof}}$ )
- Roof thermal specific capacitance ( $\kappa_{\text{roof}}$ )
- Wall thermal specific capacitance ( $\kappa_{\text{wall}}$ )
- Floor thermal specific capacitance ( $\kappa_{\text{floor}}$ )
- $g$ -value for glazing systems ( $g$ -value)

Starting from the base model described in Sect. 3, each parameter is perturbed by applying a  $\pm 10\%$  variation in the original value.

Figure 5 shows the  $s_{\%}$  sensitivity index, respectively, for HDH<sub>18</sub> and CDH<sub>26</sub> (Fig. 5a) and for minimum and maximum zone air temperature (Fig. 5b).

Note that for CDH<sub>26</sub>,  $g$ -value and roof thermal transmittance are the most influent parameters. Besides, for these variables, the indices have a positive sign that indicates a direct correlation. The greater the input values the higher the CDH<sub>26</sub> and, consequently, the cooling demand. The other indices are negative but the magnitudes of sensitivity index are close to zero. The graphs highlight the role



**Fig. 5**  $S_{\%}$  for zone heating and cooling degree hour and for minimum and maximum zone air temperature

of thermal capacitance both of wall and roof in keeping down the cooling demand. Besides, it is interesting to note the negative correlation between  $CDH_{26}$  and the wall thermal transmittance, it means that, for the test case, the night heat losses prevail on the inward heat losses.

On the other hand, Fig. 5b shows that thermal capacitance of the envelope strongly affects both minimum and maximum temperature for the investigated test case. Lower magnitude is registered for the other parameters and in particular it is interesting to note the low effects of  $g$ -values with respect to envelope capacitance.

These graphs show to which parameters the model simulation is more sensitive. Additionally, the factorial analysis method provides information on the high-order effects and then on the interactions among different parameters. The main difference is hence the simultaneous perturbation of the parameters aiming to discover the possible synergistic effects of variable perturbations. Besides, in order to compare the results both for degree hour indices and for internal peak temperatures, also the relative factorial factors are used. These indices are calculated by dividing the results of the Eqs. (6–9) for the unperturbed energy demand. The results obtained (Table 3) are consistent with the DSA.

Regarding first-order effects, the FM confirms that  $HDH_{18}$  and  $CDH_{26}$  are less affected by thermal capacitance of floor, whose index is of an order of magnitude lower than  $F_{kwall}$  and  $F_{g-value}$ .

The results of factorial analysis show weak second-order effects, and the link among variables has generally a negative sign, which means that there is not a synergistic effect. Therefore, the assumption of perfect independent variables of the DSA approach has been proved for this particular energy model. Starting from these considerations, the model can be refined by further investigating the most sensitive parameters. Moreover, also in model calibration, particular attention will be paid to the investigation of the parameter with the highest sensitivity indexes.

**Table 3** Relative factorial indexes

Effect	CDH <sub>26</sub>	HDH <sub>18</sub>	<i>t</i> <sub>max</sub>	<i>t</i> <sub>min</sub>
<i>F</i> <sub>κf</sub>	-0.0038	-0.0009	-0.0015	0.0221
<i>F</i> <sub>κw</sub>	-0.0302	-0.0042	-0.0145	0.1827
<i>F</i> <sub>g</sub>	0.0715	-0.0169	0.0138	0.0314
<i>F</i> <sub>κf-κw</sub>	0.0004	0.0001	0.0000	0.0000
<i>F</i> <sub>κf-g</sub>	0.0000	0.0000	-0.0001	0.0000
<i>F</i> <sub>κw-g</sub>	-0.0007	-0.0001	-0.0004	0.0018
<i>F</i> <sub>κwκfg</sub>	0.0000	0.0000	0.0000	0.0000

## 5 Collecting Input Data

The data gathering is a critical and complex step. Because of the large amount of parameters and inputs that affect the model, the number of missing data could be significant. Therefore, each experimental campaign is affected by a certain level of approximation, whose extent has to be established at preliminary level according to the general accuracy needed for the model.

Moreover, the data collection depends on the kind of simulation to be carried out: transient simulations reproduce detailed results, but in situ measurements are necessary to define the trends of parameters along the simulation period. On the other hand, quasi-steady state models use monthly data with a lower level of reliability in the simulation of real building behaviour.

Raftery et al. [13, 14] propose the definition of a source hierarchy for each calibration: it assigns a level of accuracy to an input data according to the reliability of the source evidence. In particular, a general hierarchy for a building simulation, as indicated also in the Guidelines ASHRAE 14 [21], is composed by:

- Direct sources
  - Long-term monitoring (>6 months)
  - Short-term monitoring
  - Spot measurement
  - Direct relief of the internal environment
  - User interview
- Indirect sources
  - Design project and documentation
  - Technical sheet of materials and operating manual of the HVAC system
- Standard sources
  - Technical standards
  - Standard guidelines and reference catalogues

In case of low-level sources and indirect investigations, spot measurements and visible inspections are necessary to verify the reliability of documentation.

Standard references represent useful tools to integrate the building model data, but they provide for general information not related to the specific building. Hence, they could be a potential discrepancy source for the building simulation.

Moreover, in a calibration process, the source hierarchy represents an important reference to refine the building simulation.

In the further sections, some measurement techniques and example of data gathering are reported.

## ***5.1 Experimental Data for Model Calibration***

In order to calibrate the building energy model, the simulation predictions have to be validated and verified against experimental measurements. Generally, the protocols and regulations indicate the actual fuel or power consumption of energy system as comparative data for model calibration. However, it is not always possible to trace the actual energy consumption, as for disused buildings or in constructions without energy systems. Therefore, in these cases, the indoor air temperature as well as the envelope surfaces temperatures may be employed as control variables for the model calibration.

The experimental data collection becomes then a key aspect in the calibration process of an energy model and, at the same time, it can be one of the most complex and expensive topic in the energy analysis. For these reasons, every in situ measurement must be based on a design of experiment established in early stage of the analysis. This document has to define the measurements with respect to the energy simulation requirements and, in particular, for the inputs highlighted by SA or for data that the energy modeller believes affected by epistemic uncertainty. The design of experiment has to define the instruments' requirements in terms of accuracy and precision, the maximum sample rate, the data quality control and assurance, the expected range of experimental data, the procedures for detection and management of outliers and missing data.

The following paragraphs will discuss some of the most frequents experimental activities carried out for the calibration of building energy models.

## ***5.2 Thermal Conductance Measures***

The measurement of envelope thermal conductance is to a large extent one of the key measures for the energy simulation refinement. Indeed, in constructive elements in which the materials are unknown, the uncertainty in the estimation of the overall conductance can be propagated through the energy model.

The standard ISO 9869:1994 [29] defines the main aspects concerning the experimental approach: it indicates the equipment to be used, methods of measurement and the quality assurance and the post-processing techniques.



Specifically, the ISO 9869 methods are valid for opaque elements characterized by normal heat flow with negligible lateral heat flows.

The measurement has to be carried out by means of one heat flow meter on the internal side (i.e., the side adjacent to the most stable temperature) and two thermometers positioned both on the internal and external surface of the wall. The heat flow meter is a thermopile of known thermal conductivity that measures the temperature difference between the two faces of the plate. Moreover, a thin silicon paste is added between heat flow meter and wall surface aiming to decrease the contact thermal resistance.

The standard sets out the measurement conditions to be met in order to ensure the reliability of results. In addition, the sampling rate and the test duration are also defined as a function of the wall characteristics, temperature trends and the post-processing method. The minimum test duration has to be greater than 72 h. However, if the temperature or the heat flux has a variable trend over time, the duration must be extended for a period longer than 7 days, until stable results are reached.

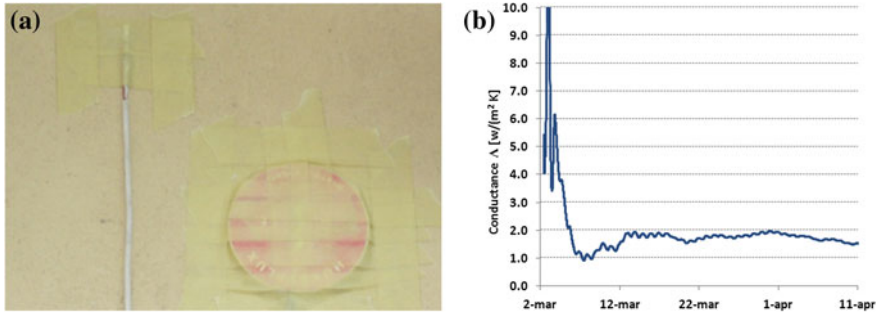
Two different post-processing techniques are proposed in the international standard, i.e., the average method and the dynamic analysis method. The average method computes the thermal conductance of the building element as the ratio of the mean density of heat flow rate over the mean temperature difference, as reported in Eq. (12).

$$A = \frac{\sum_{j=1}^N (q_j)}{\sum_{j=1}^N (\theta_{si,j} - \theta_{se,j})} \tag{12}$$

If the conductance value is estimated after each measurement, it converges to an asymptotical value (Fig. 6b). On the other hand, with the purpose of ensuring a faster solution convergence, the standard suggests the use of dynamic analysis method. Starting from the temperatures and the heat flow collected, at each time the heat flow rate can be obtained from (13):

$$\begin{aligned} q_i &= A(\theta_{si,i} - \theta_{se,i}) + K_1 \dot{\theta}_{si,i} - K_2 \dot{\theta}_{se,i} \\ &+ \sum_g P_g \sum_{j=i-p}^{i-1} \theta_{si,j} (1 - \beta_g) \beta_g (i - j) \\ &+ \sum_g Q_g \sum_{j=i-p}^{i-1} \theta_{se,j} (1 - \beta_g) \beta_g (i - j) \end{aligned} \tag{13}$$

where  $K_1$  and  $K_2$  and  $P_g$  and  $Q_g$  are dynamic characteristics depending on the  $g$  time constants  $\tau_g$ . The variables  $\beta_g$  are exponential functions of the time constants. Since Eq. (13) is a function of the  $2g + 3$  unknowns, at least  $2g + 3$  data points are needed for the solution of the linear systems. However, with the purpose of eliminating stochastic variations, an over determined system of  $M$  equations is usually solved by means of least square fit. The accuracy of the outcome of this



**Fig. 6** Thermal transmittance evaluation: **a** Heat flux meter and Pt100 position. **b** Thermal conductance evaluated by Standard ISO 6946

method is a function of the number of data analysed ( $N$ ), of the choice of the number ( $g$ ) and ratio ( $r$ ) of time constants and of the dimension ( $M$ ) of the linear system [2].

### 5.2.1 Example

The two post-processing methods are applied on the measures collected to a wall of the test case presented in Sect. 3. In particular, due to the massive wall and to the high temperature variation also at the internal side of the component, the measurement period is extended for more than a month in order to ensure the convergence of the solution. In Fig. 6a, the positions of the thermoresistance (Pt100) and of the heat flow meter both on the outer side of the wall are shown.

The first post-processing technique is the average methods applied to the measurement period that met the conditions:

- $\Lambda_{\text{END}} - \Lambda_{24} < 5\% \Lambda_{\text{END}}$ ;
- $\Lambda_{\text{END}} - \Lambda_{2/3} < 5\% \Lambda_{\text{END}}$ ;

where  $\Lambda_{\text{END}}$  is the final thermal conductance,  $\Lambda_{24}$  and  $\Lambda_{2/3}$  are respectively the conductance obtained at 24 h before the end of the monitoring and at 2/3 of the same.

The second result is obtained applying the dynamic method described in the previous section (Eq. 13) (Table 4).

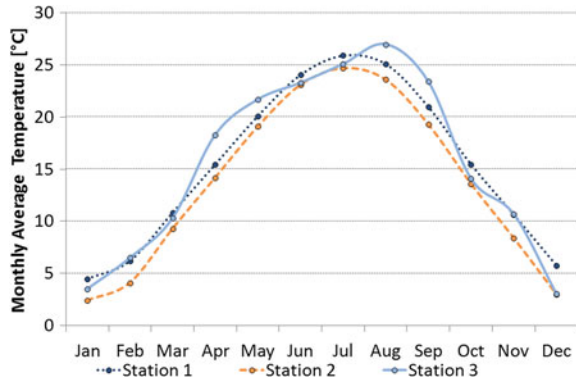
## 5.3 Weather Data for Model Calibration

Weather data represent one of the main external forces driving the building energy behaviour. Therefore, it is important to refer both the actual energy consumption and the indoor environmental variables to the actual weather conditions [17].

**Table 4** Conductance values obtained by two post-processing methods

Average method	Dynamic analysis method
1.552 W/(m <sup>2</sup> K)	1.439 W/(m <sup>2</sup> K)

**Fig. 7** Monthly average temperatures in Pavia meteorological stations



These climate conditions are then used as boundary conditions for the energy model in order to obtain consistent result with respect to measurements.

Furthermore, it should be stressed that weather data are not independent variables but rather a single set of cross-correlated measures collected at the same site location [4]. Additionally, the sample rate must be consistent with the model undertaken and, therefore, with the phenomena variability coupled with building or system response.

The data required for calibration can be obtained from meteorological stations located close to the building or directly measured in situ through the installation of a weather station. In fact, the suitability of data collected at meteorological stations cannot be taken for granted since the representativeness of local conditions are not assured owing to local climate effects such as urban heat island, urban canyons, or orographic influences [3].

As an example, Fig. 7 shows the dry bulb temperature collected in 2011 for the city of Pavia (Italy). Three meteorological stations are available in the province as shown in Table 5.

The trends of average monthly temperatures show noticeable deviations between the data recorded in different parts of the same city. This spread is mainly related to the effects of urban heat island and, consequently, to the interactions with the surrounding of meteorological station.

Therefore, it is important to correctly verify the data prior to use it in the model calibration process. In this regard, it is useful to distinguish two different stages of validation process. As defined by the guide WMO n. 8 [32], they are the quality assurance and quality control.

**Table 5** Weather data stations

Station	Context	Coordinate
1	Urban	45° 11' 42.56'' N, 9° 9' 48.42'' E, 79 m asl
2	Suburban	45° 10' 51.331'' N, 9° 8' 48.053'' E, 55 m asl
3	Urban (city centre)	45° 11' 8.931'' N, 9° 9' 28.463'' E, 87 m asl

1. *Quality assurances* are all the planned and systematic activities implemented within the quality system to provide adequate confidence that an entity will fulfil requirements for quality. The primary objective of the quality assurance system is to ensure that data are consistent, meet the data quality objectives and are supported by comprehensive description of methodology.
2. *Quality controls* are the operational techniques and activities that are used to fulfil requirements for quality. The primary purpose of quality control of observational data is missing data detection, error detection and possible error corrections in order to ensure the highest possible reasonable standard of accuracy for the optimum use of these data by all possible users.

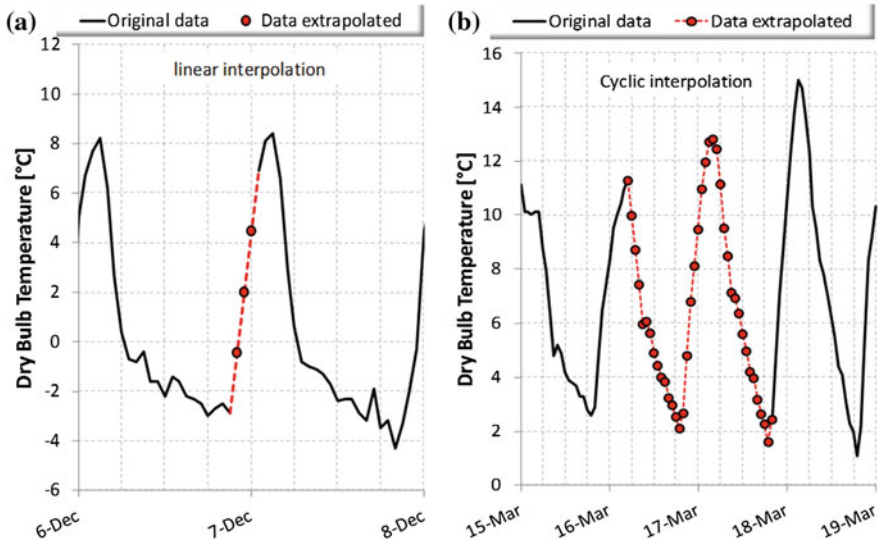
These two definitions clearly indicate that, when data are obtained from meteorological stations, the quality assurance activities are the responsibility of the owner of the station, while the verification of raw data (quality control) can be charged to the end user. On the other hand, the energy modeller has to ensure the quality assurance in case of data obtained from an in situ weather station specifically installed for the purpose.

The quality control activities aim to discover the outliers and the unphysical data. In this regard, the WMO guide suggests these checks [1]:

- values exceeding more than 50 % the 1st and 99th percentile are deleted;
- temperature derivatives higher than 4 K/h are not physical;
- values repeated for more than five times for temperature, solar radiation and wind velocity are anomalous data;
- values repeated for more than five times for relative humidity are anomalous if lower than the 75th percentiles;
- global solar radiation higher than solar constant are eliminated as well as radiation before sunrise or after sunset;
- negative values of wind velocity, solar radiation and relative humidity as well as relative humidity higher than 100 % are unphysical.

The data that do not meet these requirements are deleted and treated as missing values in the interpolation phase. In addition, it is generally assumed a threshold of 25 % [23] of missing data in a specific measurement period to prevent that the excessive interpolation leads to the use of a synthetic dataset.

The use of linear interpolation is not always the best solution for data filling. In fact, the use of linear interpolation for temperature, relative humidity and wind velocity can be accepted for short period of missing data [12]. For longer period and for solar radiation, the linear interpolation cannot adhere to the natural



**Fig. 8** Weather data interpolation: **a** Linear interpolation. **b** Cyclic interpolation



variation in the weather data. Therefore, in these cases, a cyclic interpolation is generally used (Fig. 8).

Lastly, it is important to remember that the weather data must comply with the energy model requirements. For example, if the energy analysis is performed by means of an hourly dynamic simulation, the main weather data required are the following [18]:

- Global horizontal irradiance: is the total amount of direct and diffuse solar radiation received on a horizontal surface during the 60-min period ending at the time stamp
- Dry bulb temperature: is the dry bulb temperature at the time indicated (instantaneous value)
- Relative humidity: is the relative humidity at the time indicated (instantaneous value)
- Wind velocity: is the wind speed at the time indicated (instantaneous value).

Therefore, particular attention should be paid when data collected in meteorological station are used. In fact, weather variables are routinely sampled with temporal frequencies of 10–15 min, while the published data are generally hourly average values. Therefore, the instantaneous values must be requested for temperature, relative humidity and wind speed whereas the adopted average techniques has to be investigated for the solar radiation values. In fact, there are no widely accepted standard and, consequently, each institution uses its own convention such as a forward, backward or centred average (Table 6).

**Table 6** Evaluation of hourly average

Backward average		Forward average	
Measurements	Time stamp	Measurements	Time stamp
06:00		06:15	
06:15		06:30	
06:30		06:45	
06:45		07:00	

## 6 Evaluation of Actual Energy Consumption

The actual fuel consumption is a reference for the calibration that allows to compare the real behaviour with the model results in terms of energy demand of the energy systems. This section describes some methods for the gathering of data consumption and for the data post-processing.

In particular, the actual energy needs are evaluated basing on the amount of fuel (by volume or weight) converted in energy through multiplication by the lower heating value according to the following relationship:

$$Q_{\text{real}} = V_{\text{fuel}} \cdot \text{L.H.V.} \quad (14)$$

where

- $Q_{\text{real}}$  → actual energy needs
- $V_{\text{fuel}}$  → fuel amount di
- L.H.V. → lower heating value<sup>2</sup> (reference values are reported Table 7).

The total energy consumption of a building consists in several components:

$$C_{\text{coll}} = C_h + C_W + C_{\text{cook}} \quad (15)$$

where

- $C_{\text{coll}}$  → real gathered consumption
- $C_{o_h}$  → heating  $C_{o_h} = C_{o_h} = 0$  (during summer season)
- $C_{o_W}$  domestic hot water production
- $C_{\text{cook}}$  → for cooking

In Table 8 reference values for cooking energy needs for residential buildings are presented; these terms can be assumed as constant during all the monitoring period.

<sup>2</sup> Generally, only the H.H.V. (higher heating value) is reported in the utility bills. Nevertheless, L.H.V. is required to obtain effective energy consumption. Therefore LHV has to be estimated starting from the HHV.

**Table 7** Reference lower heating values for common fuels

Fuel	Low heating value (L.H.V.)
Methane	9.940 kWh/Nm <sup>3</sup>
Propane	28.988 kWh/Nm <sup>3</sup>
Butane	36.779 kWh/Nm <sup>3</sup>
Diesel fuel	11.870 kWh/kg

**Table 8** Reference coking energy needs

Plan surface (m <sup>2</sup> )	Specific energy need (kWh/G)
<50	4
50 m <sup>2</sup> < Surface < 120 m <sup>2</sup>	5
>120 m <sup>2</sup>	6

In addition, it is necessary to divide the energy needs for heating respect to domestic hot water requirements, which can be deducted through summer measurements, (after the cooking contribute subtraction).

In fact, energy needs for domestic hot water are assumed to be fixed throughout the year with an adequate level of approximation, if thermal solar systems are not installed. Hence the summer DHW consumptions can be used even for winter.

Another method to deduce domestic hot water, cooking and plug loads is based on the correlation between external temperature and energy consumption during the operational period of HVAC system [20]. In fact, when the load line becomes parallel with the *x*-axis, fuel consumptions are not affected by external temperature and the constant value represents the energy needs for the production of domestic hot water and for cooking. The values for a reference year could be represented in a graph in association with monthly temperatures: the lower the external temperature, the higher the heating consumption and vice versa. When there are no fuel consumption caused by domestic hot water (electrical production), the constant value is close to zero. Also the electrical requirements trend could be expressed with respect to the monthly external temperature. The slope increases according to the temperatures owing to the cooling system consumptions. In this regard, an horizontal line represents the sum of domestic hot water, lighting and plug loads.

### 6.1 Case Study: Utility Bills Analysis

The case study is a residential detached building with a floor surface of 120 m<sup>2</sup> heated by means of a combined boiler (heating and domestic hot water). The actual fuel consumption, collected during a whole year, is reported in Table 9.

**Table 9** Real fuel demand of the case study

Reference period of the utility bills	Number of days	Fuel consumption (m <sup>3</sup> )	Energy needs (kWh)
January	30	660.00	6,560.4
February–March	59	1,178.00	11,709.32
April–May	60	425.00	4,224.5
June–August	91	169.00	1,679.86
September–November	90	1,274.00	12,663.56
December	30	213.00	2,117.22

**Table 10** Real energy needs (without cooking contribution)

Reference period of the utility bills	Number of days	Energy needs (kWh)	Cooking energy needs (kWh)	Net energy needs (kWh)
January	30	6,560.40	180	6,290.94
February–March	59	11,709.32	354	10,361.32
April–May	60	4,224.50	360	3,745.22
June–August	91	1,679.00	546	1,133.86
September–November	90	12,663.56	540	11,139.50
December	30	2,117.22	180	1,957.10

Utility bills report the fuel consumption, which can be converted into energy need through the Lower Heat Value that, for methane, is roughly equal to 9.940 kWh/m<sup>3</sup>:

$$Co(\text{kWh}) = Co(\text{m}^3) (\text{m}^3) \times 9.940 \text{ kWh/m}^3$$

This equation has been applied to obtain the values in the fourth column (Table 9). Nevertheless, cooking energy needs and the contribution for domestic hot water have to be separated from the total consumption. Considering the floor surface and the reference values reported in Table 8, the energy requirements for cooking accounts for 6 kWh/day (Table 10).

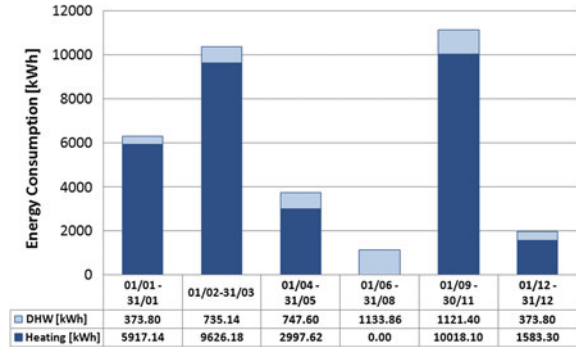
The last contribution to be separated from the total consumption is the energy required for domestic hot water preparation. Considering the average energy consumption registered from period between June and August, the daily energy needs are evaluated as:

$$\frac{1,679 \text{ kWh}}{91 \text{ g}} = 12.46 \text{ kWh/day}$$

Extending this value to the whole period, the results showed in Fig. 9 are obtained.



**Fig. 9** Heating and domestic hot water consumption



### 6.2 Source for Real Consumption Monitoring

According to the fuel of the HVAC system, different sources of data are necessary to evaluate actual consumption.

For instance, in case of network gas systems, monitoring device are installed to evaluate the consumption and define the amount of the utility bills.

There are two main methods for the data record:

- *Indirect*
- *Direct*

In the first case, real consumption is estimated through the values on the utility bills in relation to the monitoring period. Nevertheless, these amounts could be determined by a statistical evaluation according to the previous consumption (estimate values). Therefore, they cannot reproduce the real energy behaviour of the building, but they show the historical trends of fuel supply. Hence, in order to calibrate the model, the effective energy needs have to be adopted.

On the other hand, the direct method is featured by a relief of the measurement device during the monitoring period. The finer the gathering interval, the more accurate the calibration.

In case of HVAC system fuelled by a storage volume with a measurement device, the model can be calibrated considering the instrument error. If the storage has no counter, the fuel consumption can be estimated through the following equation:

$$CQ = (CQ_I - CQ_F) + CQ_A \tag{16}$$

where

- $Q \rightarrow$  quantity in the storage
- $Q_I$  initial quantity
- $Q_F$  final quantity
- $Q_A$  supplied quantity during the monitored period.

**Fig. 10** Measurement of water flow in HVAC subsystems



### ***6.3 Subsystem Consumption Measurement***

In order to calibrate enhanced simulation models, the final fuel consumption may not be suitable for the overall HVAC models. Therefore, in these cases, it is also necessary to measure the energy consumption of the HVAC subsystems up to the single components. For this purpose, it can be useful to highlight the mode and the main tools employed for the measurement of thermal and electrical energy flows. These experimental activities are already widely spread in the Anglo-Saxon world as a phase of the commissioning process, during the post-occupancy investigations [22].

In order to quantify the thermal energy flow, the measurement of air/water flow and temperature difference is required (Fig. 10). For example, the heating provided by a radiator is computed starting from the water mass flow rate and the temperature difference between inlet and outlet sections. Therefore, the energy meter already installed in central heating/cooling systems as well as, ad hoc flow meters can be installed for high-rise residential buildings. These electronic energy flow meters offer accuracy up to 1 % as reported in the calibration datasheet.

As regards the measurement of the current in auxiliary systems, the most common instruments are the current transducer (CT). These instruments are placed on wires connected to specific auxiliary system such as motors, pumps or lights and then connected to a digital multi-meter. The CT has typical accuracy up to one per cent. If coupled with the voltage monitoring, by means of a voltmeter, this measure can be used to estimate the appliance power consumptions. However, separate voltage and current measurements should not be used for inductive loads such as motors or magnetic ballasts [27]. In fact, if the signal is distorted owing to

various noise sources, a transducer (true RMS) must be adopted. These instruments are capable of accurate measurements of AC voltage even if the waveforms are not purely sinusoidal.

## 7 Measure of Air and Surface Temperature

The temperature measurement devices commonly used are resistance thermometer (RTD), thermistors and thermocouples. These tools do not directly measure the temperature but rather the variation in a quantity related to the temperature changes. In addition to the different measured variable, these thermometers differ from each other for the cost, the accuracy and the range of measurement. Therefore, the use of a thermometer with respect to another depends on the particular conditions of the temperature to be measured.

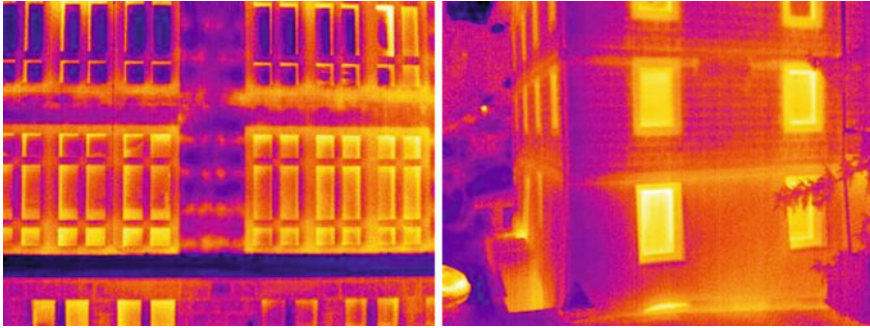
The RTD represents one of the most common types of thermometer. In these instruments, the temperature variations are related to the changes in electrical resistance of metal. Platinum RTDs, usually Pt100 or Pt1000, are remarkable instruments: the Pt100 sensor has a resistance of 100 ohm at 0 °C and it is by far the most common type of RTD sensor. These sensors are normally covered by some protective sheath or mounting to form probes that are commonly referred as platinum resistance thermometer (PRT). The tolerances for PRT sensors are specified by the International Standard IEC 751:1983<sup>3</sup>. In this standard, two classes are defined: Class A, with a tolerance of  $\pm 0.15$  °C at 0 °C; and Class B, with a tolerance of  $\pm 0.3$  °C at 0 °C. Sometimes the accuracy classes provided by the manufacturer are defined as 1/10 DIN or 1/3 DIN. This means, respectively, a certified tolerance of 1/10 or 1/3 of the Class B specification. The linear relation between platinum resistance and temperature, in the range of environmental temperatures, makes them the thermometer of choice for many applications. The main limitation of this type of sensors is connected to the relative higher cost, from 20 to 300 €, linked to the metal cost.

For this reason, RTDs using semiconductors in lieu of metals (i.e., bulk semiconductor sensor or thermistors) are also very popular. Additionally, the semiconductor material exhibits a large change in resistance proportional to a small change in temperature. Besides, thermistors are one of the most accurate types of temperature sensors with a typical accuracy of  $\pm 0.1$ – $0.3$  °C depending on the particular thermistor model. However, thermistors are fairly limited in their temperature range (typical 0–100 °C) and in the non-linear relation temperature resistance against the lower cost from 0.20 to 20 €.

However, to a considerable extent, the cheaper and widespread thermometer in temperature measures is the thermocouple. This instrument is based on the Seebeck's effect, whereby if two conductors of different material are jointed, a current

---

<sup>3</sup> DIN IEC 751:1983, Temperature/Resistance Table for Platinum Sensors



**Fig. 11** Thermography analysis of an external wall

grows proportional to the temperature difference of the two joint. A thermocouple is available in different combinations of metals or calibrations. The most common in building analysis are type T for environmental temperature and type K for high temperature measurements, such as HVAC systems. Although for the most precise measurements, the reference joint should be kept in a triple point of water, however, such accuracy is rarely needed and a multi-meter reference joint can be adopted.

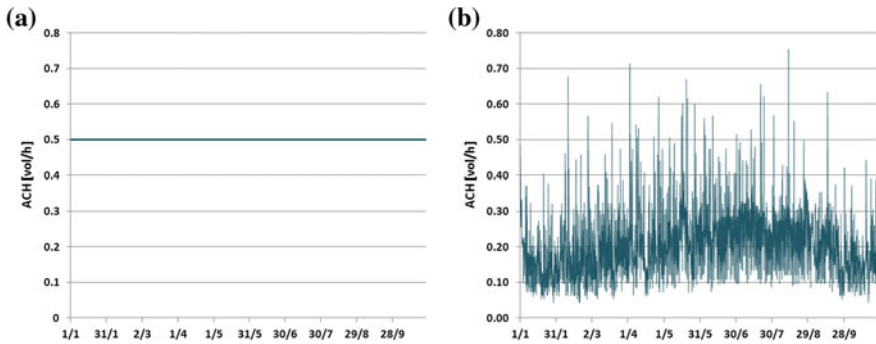
Nonetheless, the low accuracy frustrates the advantage of the limited cost, from 0.80 to 3 € as a function of the wire insulation and shelter. The EN 60584-2 [25] standard defines the accuracy requirement tolerance that for type T thermocouple are within  $\pm 0.5$  °C for first class and  $\pm 1.0$  °C for second class.

Starting from the instrument choice, the correct installation position has to be checked, thus ensuring that the boundary conditions do not influence the measurement. For this reason, the instruments must not be placed close the heat sources or direct exposed to sunlight or drafts. Furthermore, for the surface temperature measurements, the position must avoid the edge effects due to the presence of thermal bridges or to non-homogeneous area. For this purpose, the surface should be checked by means of a thermography survey with the purpose of detecting any structural discontinuities or areas with high moisture content (Fig. 11).

## **8 Building Model Input and Experimental Calibration: Analysis on a Case Study**

According to the results of the SA, some parameters were investigated by experimental analysis and more accurate evaluation in order to refine the model.

In particular, the thermophysical properties of the envelope are evaluated both through standard and in situ measurements. The external wall in zone P3\_Z1 is 65 cm thick, it has a high thermal mass and it is composed by bricks and sand. Therefore, according to the Italian technical specification UNI TS 11300-1, the



**Fig. 12** a Standard air-change rate (0.5 vol/h). b Calculated air-change rates (EN 15242)

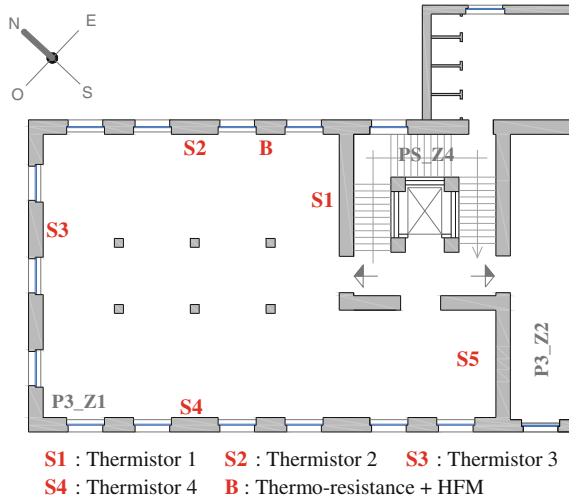
reference structure CO-01 is chosen. Moreover, an experimental analysis is carried out conforming to ISO 9869. Two couples of HFM and thermo-resistance Pt100 are positioned both on internal and external surfaces in order to measure surface temperatures, inward and outward heat fluxes. The measurements are carried out for 70 days (2<sup>nd</sup> March–10<sup>th</sup> May) in order ensure the convergence of the solution.

The monitored data are post processed with the average method described in standard ISO 9869. The values of conductance for standard and experimental method are, respectively, equal to 1.372 and 1.552 W/(m<sup>2</sup> K).

Furthermore, considering the absence of HVAC system and the leakages of the envelope, infiltration losses represent a significant contribution. Figure 12a, b show the different air-change rates applied for model definition. Since the envelope presents numerous cracks and leakages, the standard value 0.5 ACH is adopted even if it is used for global natural ventilation. EN 15242 [26] defines a standard method to estimate the infiltration air-change rates, according to envelope features and to local weather data (temperature and wind speed).

In Fig. 13, the instrument position is shown: the heat flux meter (HFM) apparatus (two HFM and two thermoresistance Pt100) is installed in B, while the points from S1 to S5 indicate the thermistors employed for the surface temperature recording. Since the building has no HVAC system, the internal temperatures have been monitored in order to calibrate the simulation model. In particular, both the surface and air temperatures were collected every 10 min in the control thermal zone (i.e., P3\_Z1) that is placed on the 4<sup>th</sup> floor, next to the roof (Fig. 13). The measurement campaign was carried out from March to October 2012.

Starting from the described sources of input data, a series of simulations is carried out with the software TRNSYS (TRNSYS: A Transient Simulation Program, Ver. 16, University of Wisconsin-Madison, 2007). A code identifies each model and it describes which kind of parameter is applied in the analysis. Table 11 reports the set of simulations and it explains which inputs are implemented.



**Fig. 13** Control thermal zone: monitoring devices

**Table 11** Set of simulations

Simulation	Air-change rates		Thermal conductance	
	0.5	EN 15242	Standard	Measured
tn_05_std	x		x	
tn_05_ms	x			x
tn_en_ms		x		x

## 9 Validation Indices

### 9.1 Calibration with Real Consumption

In case of model calibration with real consumption of buildings, for both electrical and fuel energy needs, the reference statistical indices are presented in ASHRAE Guidelines 14/2002 [21]. They assess the discrepancies between real and predicted values.

#### 9.1.1 Mean Bias Error $MBE_{\%}$

Mean bias error is evaluated by summing the differences between measured consumptions ( $M$ ) and predicted energy needs ( $S$ ) along the considered time interval and dividing each difference for the corresponding measured value in order to obtain a percentage index.

$$\text{MBE}_{\%} = \left[ \frac{\sum_{i=1}^n (M_i - S_i)}{\sum_{i=1}^n (M_i)} \right] \quad (17)$$

$\text{MBE}_{\%}$  provides for a general assessment of the simulation reliability, in relation to the actual behaviour monitored during the in situ measurement. In addition, it allows to evaluate whether the model overestimates or underestimates the real energy needs. Nevertheless,  $\text{MBE}_{\%}$  is not adequate to validate a simulation, because it can give misleading indications due to the sign error compensations. In fact, opposite sign errors tend to neutralize each other and they are not highlighted in the final result. For this reason, additional indices are needed.

### 9.1.2 Cumulative Variation in Root Mean Square Error

This index is based on the standard deviation between actual ( $M$ ) and simulated ( $S$ ) behaviour.

$$\text{RSME}_{\text{period}} = \sqrt{\frac{\sum_{\text{period}} (M - S)_{\text{period}}^2}{N_{\text{period}}}} \quad (18)$$

The Root Mean Square Error determines the absolute value of the discrepancies between two parameters, and it assesses the effectiveness of the simulation in comparison with the real behaviour. The higher the RMSE value, the lower the reliability of the model. However, in case of calibration with real energy consumption, RMSE could be inadequate: in fact the same value of RMSE could be associated both to an accurate model with high consumption and to an inaccurate model with low energy consumption. Therefore, the cumulative variation in RMSE is assumed because it expresses the percentage deviation in relation to a mean value of measured energy needs.

$$\text{CV}(\text{RSME}_{\text{period}}) = \left[ \frac{\text{RSME}_{\text{period}}}{A_{\text{period}}} \right] \times 100 \% \quad (19)$$

where  $A_{\text{period}}$  is an average value based on the number of intervals that characterizes the measurement period:

$$A_{\text{period}} = \left[ \frac{\sum (M_{\text{period}})}{N_{\text{period}}} \right] \quad (20)$$

### 9.1.3 Calibration Criteria

The number of measurement intervals depends both on the reference period of the monitoring and on the kind of simulation carried out: in case of steady state

**Table 12** Tolerance ranges

Index	IPMVP (%)	M&V (%)	ASHRAE 14 (%)
MBEmonthly	±20	±15	±5
CV (RMSEmonthly)	5	10	15
MBEhourly	–	–	±10
CV(RMSEhourly)	–	–	30

models the calibration is fulfilled through monthly data, while for transient models through hourly or sub-hourly data.

The calibration criteria and the tolerance range have to be established at early stage in relation to the availability of data, the simulation type and the detail level request for the assessment.

The evaluation protocols set different values depending on the model type: for hourly simulations 30 % of discrepancies in terms of CVRMSE and 10 % in terms of MBE are considered acceptable, whereas for the simulations calibrated on monthly data, the tolerance range is halved (Table 12).

## 9.2 Calibration with Temperature

The model calibration through the temperature monitored in a control thermal zone requires error indices that provide significant indication in terms of temperature discrepancies between predicted and real values.

### 9.2.1 Mean Bias Error MBE

$$\text{MBE} = \left[ \frac{\sum_{i=1}^n (M_i - S_i)}{N} \right] \quad (21)$$

The average error MBE is the sum of the differences between measured ( $M$ ) and simulated ( $S$ ) temperatures along the monitoring period divided by the number of records. A positive value of MBE indicates that the model overestimates the temperatures, while a negative value of MBE represents an underestimation of the internal temperature of the control thermal zone. Nevertheless, as highlighted in Sect. 9.1.1, MBE is affected by the sign error compensation, and for this reason, additional indices have to be adopted.



### 9.2.2 Root Mean Square Error

$$\text{RSME} = \sqrt{\left[ \frac{\sum_{i=1}^n (M_i - S_i)^2}{N} \right]} \quad (22)$$

Root mean square error RMSE overcomes the misleading of MBE, since it provides for the absolute value of the discrepancies between the temperatures.

### 9.2.3 Pearson's Index

For model calibration with internal temperatures, the correlation between predicted and real values is a significant indication of the simulation reliability.

The Pearson's index ( $r$ ) assesses the correlation between two variables, in this case, the temperature trends (predicted and real) and it allows to verify the reliability of simulation:

$$r = \frac{\sum(M \cdot S) - \sum M \cdot \sum S / N}{\sqrt{\left( \sum M^2 - \frac{(\sum M)^2}{N} \right) \cdot \left( \sum S^2 - \frac{(\sum S)^2}{N} \right)}} \quad (23)$$

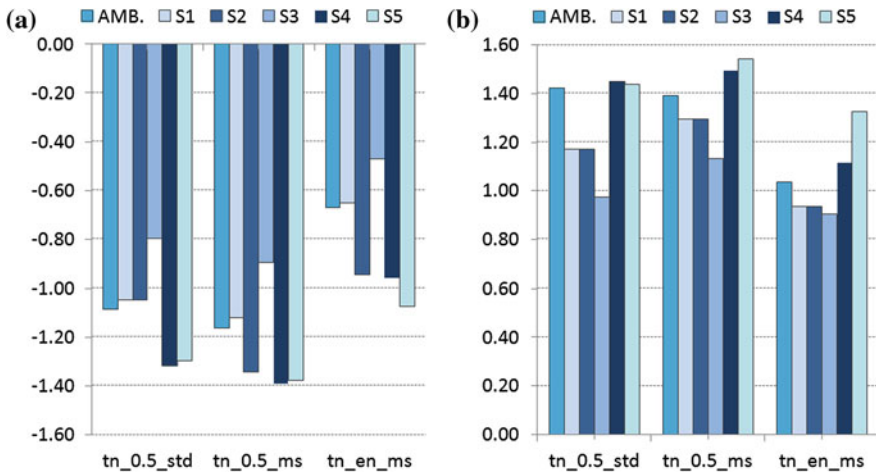
where:

- $M$  measured temperatures ( $^{\circ}\text{C}$ )
- $S$  simulated temperatures ( $^{\circ}\text{C}$ )
- $N$  number of intervals

The Pearson's index ranges from  $-1$  to  $1$ : where a negative value means an opposite correlation

- $r < 0$  opposite correlation, if the model temperature increases, the measured values trend to decrease and vice versa; therefore the model is not representative of the real building behaviour;
- $r = 0$  no correlation between variables;
- $r > 0$  direct correlation, if the model and the monitored temperatures have the same trend.  $r > 0.5$  represents a significant correlation between temperature variables [3].

The measurement precision can be considered as the reliability limit. This is possible if we consider the correct estimation of the internal temperatures for the control thermal zone aims to validate the simulation energy needs of the analysed building [9].



**Fig. 14** **a** Mean bias error for hourly temperatures. **b** Root mean square error for hourly temperatures

## 10 Model Calibration Results

In this section, the calibration process of the dynamic hourly simulation model of the test case (Sect. 3) is presented. The accuracy of the numerical model with respect to the measured data is evaluated both through the statistical indicators (i.e., MBE, RMSE and Pearson’s index) and by means of a graphically comparing between the model and experimental trends of temperatures.

The first part of the section will discuss the early stages of calibration. In particular, starting from the initial energy model, firstly the standard values of thermal conductance are replaced with those measured by the in situ tests. Following on from this point, the standard ventilation rate is replaced with the more detailed calculation procedure present in the EN 15242 [26].

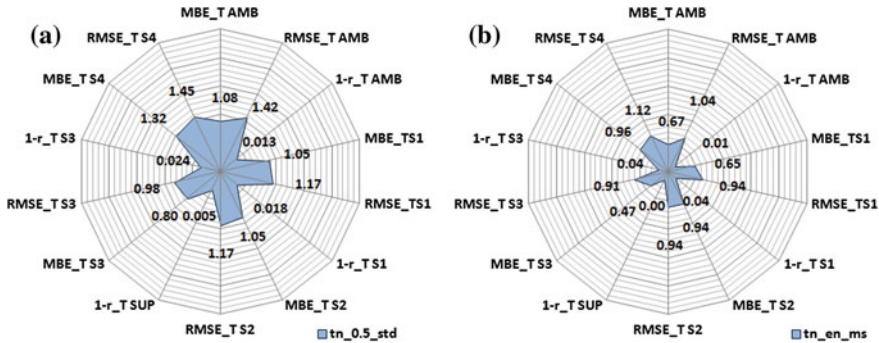
In the second part, instead, the final results of the calibration are presented. The calibration is performed by varying the parameters highlighted by the SA according to a uniform distribution, within the plausible range of variability, with the purpose of finding the parameter set that best fits the actual building behaviour. This investigation is carried out on the monitoring period from 2<sup>nd</sup> March to 22<sup>nd</sup> October 2012.

Figure 14a and b show the statistical indexes for both air (air) and the envelope surface (S1—S2—S3—S4—S5) temperature in the control thermal zone.

MBE quantifies the long-term performance of a model. A positive value represents the average amount of overestimation in the predicted values and vice versa. MBE in Fig. 14a highlights a general underestimation of the predicted temperature with respect to actual data. Besides, it clearly shows a greater convergence of the refined models with respect to the initial-based model.

**Table 13** Pearson’s indices—air temperature

tn_0.5_std	tn_0.5_ms	tn_en_ms
0.987	0.991	0.992



**Fig. 15** a Error indices for simulation try\_05\_std. b Error indices for simulation tn\_en\_ms

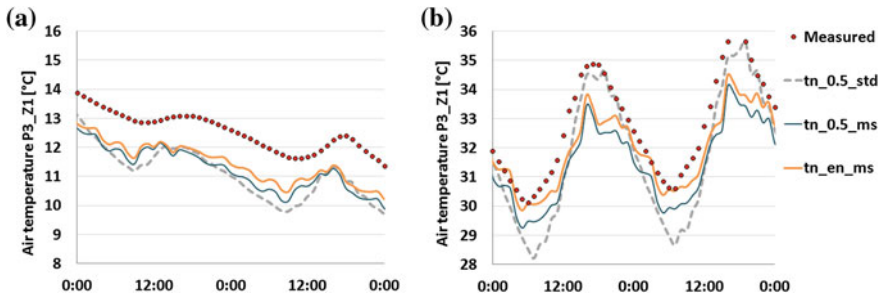
Nevertheless, MBE drawback arises from the compensation between underestimations and overestimations. Therefore, to assess the reliability of a simulation other indices are required.

In this regard, RMSE overcomes this problem, since it reveals the absolute discrepancies between actual and simulated temperatures. This parameter provides information about the short-term performance of the method by means of a term by term comparison. The smaller the RMSE value, the better are the model provisions. Figure 14b shows a slight convergence of the indexes. In fact, in this test, a few large errors can produce a significant increase in the RMSE index.

These results are also confirmed by the Pearson’s index. The values reported in Table 13 highlight as the greatest index increment is obtained using the measured thermal conductance.

Lower increment is achieved by improving the infiltration model. Nevertheless, even Pearson’s index shows some weakness. In fact, in case of general uniformity with small deviation between minimum and maximum values, Pearson’s index assumes relative high average. Consequently, also this parameter does not permit a univocal assessment of the best model combination. Therefore, a multi-criteria analysis has to be applied by simultaneously plotting the different indexes for all the temperature sensors (Fig. 15). In these pictures, the indexes are plotted for the initial and refined models by means of a radar plots representing the multi-criteria analysis according to the following indices:

- absolute values of mean bias error ( $|MBE|$ ) for air and surface temperatures (S1, S2, S3, S4, S5)
- values of root mean square error (RMSE)
- complementary values of Pearson’s Indices ( $1 - r$ ).



**Fig. 16** a Air temperature trends (March 4th–5th). b Air temperature trends (June 20th–21st)

**Table 14** Tolerance ranges

Input	Low limit (%)	High limit (%)
Infiltration rates	-20	+20
$U_{\text{roof}}$	-50	+50
$U_{\text{wall}}$	-20	+20
$U_{\text{floor}}$	-50	+50
Roof capacitance	-50	+50
Wall capacitance	-50	+50
Floor capacitance	-50	+50
$g$ -value for glazing	-30	+30

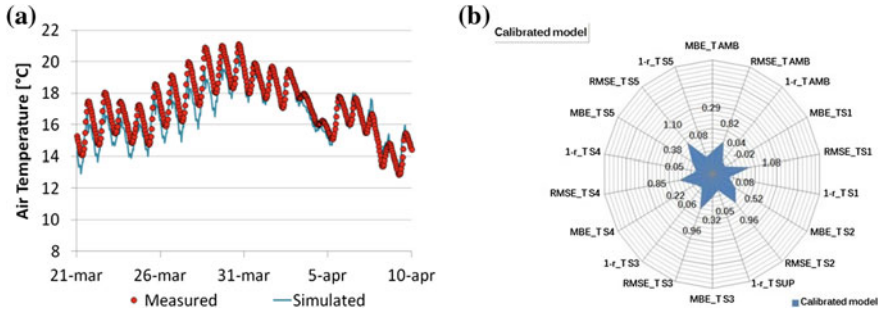
The higher the blue-painted area, the higher the discrepancies between predicted and actual values of temperatures and, therefore, the lower the reliability of the model. Moreover, this representation highlights the temperature predictions for which the model shows the greatest differences from the measured data.

Nevertheless, error indices give information about the global gap between actual and predicted temperature. A graphical comparison between the hourly trends of temperature is useful in order to have a punctual but qualitative indication of the reliability of building simulations (Fig. 16a, b).

The graphs point out some discrepancies in the evaluation either of positive and negative temperature peaks. Probably, this spread is caused by the incorrect modelling of the thermal capacitance of the walls or to the incorrect estimation of the window solar transmittance.

For this reason, the parameters investigated in the SA are simultaneously varied according to a uniform distribution in order to find the parameter set that best approximates the actual building behaviour. In particular, the range of variation, with respect to the initial value, shown in Table 14 are adopted. These take into account the real knowledge of the parameter and its expected variability.

Several hourly simulations are performed by varying the input data. The evaluation of the model convergence is performed through the multi-criteria analysis previously presented. In Fig. 17a, the internal temperature trend of the control thermal room (measured and simulated values) is reported while in Fig. 17b the radar



**Fig. 17** Calibrated model: **a** Air temperature trends. **b** Multi-criteria radar plot of the calibrated model

graphs obtained for the calibrated model is shown. After the calibration process, the indices MBE and  $r$  decrease, while RMSE values still remain high. This problem occurs because of the nature of RMSE index, whose amount is affected even by a small number of simulated points that are not consistent with real value. In fact, as it is shown in Fig. 17a, the simulation trend approaches to actual values with lower discrepancies with respect to the previous simulations. Nevertheless, the calibrated model presents some errors in the lower peak values during the winter season.

## References

1. Antonacci G, Todeschini I (2013) Derivation of meteorological reference year with hourly interval for Italy. In: Proceedings of 1st IBPSA Italy conference, January 30th–February 1st 2013, University of Bozen, Italy
2. Cappelletti F, Prada A, Romagnoni P, Baggio P (2013) Determination of roof dynamic thermal behaviour by means of in situ measurements: the post-processing analysis. In: Proceedings of CLIMA 2013—11th REHVA world congress and the 8th international conference on IAQVEC June 16–19, 2013, Prague Congress Centre, Czech Republic
3. Giovannini L (2012) Urban scale phenomena and boundary layer processes in mountain valleys. Ph.D. thesis, University of Trento
4. Guan L, Yang J, Bell JM (2007) Cross correlations between weather variables in Australia. *Build Environ* 42:1054–1070
5. Kioutsoukias I, Tarantola S, Saltelli A, Gatelli D (2004) Uncertainty and global sensitivity analysis of road transport emission estimates. *Atmos Environ* 38(38):6609–6620
6. Lam J, Hui S (1996) Sensitivity analysis of energy performance of office buildings. *Build Environ* 31:27–39
7. Lomas KJ, Eppel H (1992) Sensitivity analysis techniques for building thermal simulation programs. *Energy Build* 19(1):21–44
8. Macdonald IA (2002) Uncertainty in building simulation. Ph.D. dissertation, University of Strathclyde, Glasgow UK
9. Nicholas JV, White DR (2001) Traceable Temperatures. An introduction to temperature measurement and calibration. Wiley&sons, Chichester
10. Norford LK, Socolow RH, Hsieh ES, Spadaro GV (1994) Two-to-one discrepancy between measured and predicted performance of a ‘low-energy’ office building: insights from a reconciliation based on the DOE-2 model. *Energy Build* 21:121–131

11. Ozisik M, Orlande H (2000) *Inverse Heat Transfer - Fundamentals and applications*. Taylor and Francis, New York
12. Prada A (2012) Energy performance of buildings: modeling of dynamic summer behaviour. Ph.D. thesis, Civil and Environmental Engineering, University of Trento, Trento
13. Raftery P, Keane M, Costa A (2011) Calibrating whole building energy models: detailed case study using hourly measured data. *Energy Build* 43:3666–3679
14. Raftery P, Keane M, O'Donnell J (2011) Calibrating whole building energy models: an evidence-based methodology. *Energy Build* 43:2356–2364
15. Scollo S, Tarantola S, Bonadonna C, Coltelli M, Saltelli A (2008) Sensitivity analysis and uncertainty estimation for tephra dispersal models. *J Geophys Res B: Solid Earth* 113(6)
16. Tian Z, Love JA (2009) Energy performance optimization of radiant slab cooling using building simulation and field measurements. *Energy Build* 41(3):320–330
17. Tian W, deWilde P (2011) Uncertainty, sensitivity analysis of building performance probabilistic climate projections: a UK case study. *Autom Constr* 20(8):1096–1109
18. Wilcox S, Marion W (2008) Development of an updated typical meteorological year data set for the United States. In: *Proceedings of 37th ASES annual conference, 33rd national passive solar conference, 3rd renewable energy policy and marketing*, American Solar Energy Society—SOLAR 2008
19. Pan Y, Huang Z, Wu G, Chen C (2009) The application of building energy simulation and calibration in two high-rise commercial building in Shanghai. In: *Proceedings of IBPSA conference, International Building Performance Simulation Association, Glasgow, 2009*
20. Yoon JH, Lee EJ (2009) Calibration procedure of energy performance simulation model for a commercial building. In: *Proceedings of IBPSA conference, International Building Performance Simulation Association, Glasgow, 2009*

## Standard References

21. ASHRAE Standard Committee (2002) ASHRAE guideline 14-2002: measurement of energy and demand savings
22. ASHRAE Standard Committee (2005) ASHRAE guideline 0-2005: the commissioning process
23. ASHRAE Standard Committee (2013) ASHRAE handbook fundamentals 2013, ASHRAE
24. CEN Thermal insulation—construction products, building elements and structures. In: *Situ measurement of thermal performance—Part 4 testing of structures*, (Working group 14)
25. CEN (1993) Thermocouples—Part 2 Tolerances EN 60584-2
26. CEN (2008) Ventilation for buildings—calculation methods for the determination of air flow rates in buildings including infiltration EN 15242:2008
27. “Efficiency Valuation Organisation (2012), International Performance Measurement and Verification Protocol (IPMVP 2012)
28. European Union (2010) Directive 2010/31/EU of the European Parliament and of the council of May 19th, 2010 on the energy performance of buildings (recast). *Official Journal of the European Union*, 18 June, 2010
29. ISO (1994) Thermal insulation—building elements. In: *Situ measurement of thermal resistance and thermal transmittance*, ISO 9869:1994
30. ISO (2008) Technical specification, energy performance of buildings. Part 1. Evaluation of energy need for space heating and cooling, UNI/TS 11300-1:2008
31. US Department of Energy (2008) M&V guidelines: measurement and verification for federal energy projects 2008, US Department of Energy. <http://mnv.lbl.gov/keyMnVDocs/femp>
32. World Meteorological Organization (2008) WMO n. 8 Guide to meteorological instrument and methods of observation